Molecular Dynamics Simulations of GABA Binding to the $GABA_C$ Receptor: The Role of Arg^{104}

Claudio Melis,* Sarah C. R. Lummis,†‡ and Carla Molteni*
*Physics Department, King's College London, London, United Kingdom; †Department of Biochemistry, University of Cambridge, Cambridge, United Kingdom; and ‡Division of Neurobiology, Laboratory of Molecular Biology, Cambridge, United Kingdom

ABSTRACT GABA is the major inhibitory neurotransmitter in the nervous system and acts at a variety of receptors including $GABA_C$ receptors, which are a subclass of $GABA_A$ receptors. Here we have used molecular dynamics simulations of GABA docked into the extracellular domain of the $GABA_C$ receptor to explain the molecular interactions of the neurotransmitter with the residues that contribute to the binding site; in particular, we have explored the interaction of GABA with Arg^{104}. The simulations suggest that the amine group of GABA forms cation-π interactions with Tyr^{102} and Tyr^{198}, and hydrogen-bonds with Gln^{83}, Glu^{220}, Ser^{243}, and Ser^{168}, and, most prominently, with Arg^{104}. Substituting Arg^{104} with Ala, Glu, or Lys, which experimentally disrupt $GABA_C$ receptor function, and repeating the simulation revealed fewer and different bonding patterns with GABA, or the rapid exit of GABA from the binding pocket. The simulations therefore unveil interactions of GABA within the binding pocket, and explain experimental data, which indicate that Arg^{104} is critical for the efficient functioning of the receptor.

INTRODUCTION

$GABA_C$ receptors, which are a subfamily of $GABA_A$ receptors, are members of the Cys-loop superfamily of ligand-gated ion channels (LGICs), an important group of receptors involved in rapid synaptic transmission and whose malfunction can result in a variety of neurological disorders; hence, understanding their mechanism of action is of considerable pharmacological interest. $GABA_C$ receptors are mostly located in retinal neurons where they play a role in retinal signaling and may be involved in diseases such as macromolecular degeneration (1). The receptors are activated by the binding of GABA, the main inhibitory neurotransmitter in the central nervous system. $GABA_C$ receptors have distinct pharmacological properties from $GABA_A$ receptors, e.g., they are not inhibited by bicuculline, the classic $GABA_A$ receptor antagonist (2,3).

Like all the LGICs belonging to the Cys-loop superfamily, $GABA_C$ receptors are composed of five subunits arranged in a pentagonal array around a central ion-permeant pore. Each subunit has an extracellular N-terminal domain (ECD), a transmembrane domain composed of four α-helices, and an intracellular domain. Three subunits (ρ_{1-3}) have been identified; these can all form functional homomeric or heteromeric receptors (4). Our study is focused on the homomeric receptors consisting of ρ_1 subunits.

Due to the lack of detailed structural information for $GABA_C$ receptors, homology models of its ECD have been computer-generated using, as a template, the structures of the acetylcholine binding protein (AChBP), a protein homologous to the ECD of LGICs of the Cys-loop superfamily (5–8).

GABA binds in its zwitterionic form, with the negative charge localized in the carboxylate group and the positive charge in the amine group (9). The alleged GABA binding site, shown in Fig. 1, is at the interface between subunits and is constituted by residues associated with several noncontiguous loops (*A–F*), including several aromatic residues (Tyr^{102} in loop D, Tyr^{198} in loop B, and Tyr^{241} and Tyr^{247} in loop C), which form the classic Cys-loop receptor aromatic ''box,'' and polar and charged residues (Gln^{83}, Arg^{104} in loop D, Arg^{158} and Ser^{168} in loop E, Glu^{220} in loop F, and Ser^{243} in loop C). Docking studies indicate that the amine group of GABA is inside the tyrosine-made aromatic cage, while the GABA carboxylate group is likely to be located in between the positively charged Arg^{104} and Arg^{158} (5,6).

Mutagenesis experiments, combined with Hartree-Fock calculations, confirmed the amine orientation by identifying a cation-π interaction with Tyr^{198} (10). The roles of the charged and hydrophilic residues located in or close to the alleged binding site were also investigated by mutagenesis experiments: the results showed that two arginines, Arg^{104} and Arg^{158}, are crucial for the binding of GABA and/or for receptor function (6). In fact, the substitution of Arg^{104} with either Ala or Glu resulted in >10,000-fold increases in EC_{50}s, while the substitution with Lys resulted in nonfunctional receptors; the substitution of Arg^{158} with Ala, Glu, and Lys resulted in nonfunctional receptors.

Experimental data suggest that the orientation of GABA in $GABA_C$ receptors is subtly different from that in $GABA_A$ receptors, where the neurotransmitter has been shown to have

Submitted December 11, 2007, and accepted for publication July 1, 2008.

Address reprint requests to Claudio Melis, Tel.: 44-20-78-48-20-64; E-mail: claudio.melis@kcl.ac.uk.

Editor: David S. Weiss.

0006-3495/08/11/4115/09 $2.00

doi: 10.1529/biophysj.107.127589

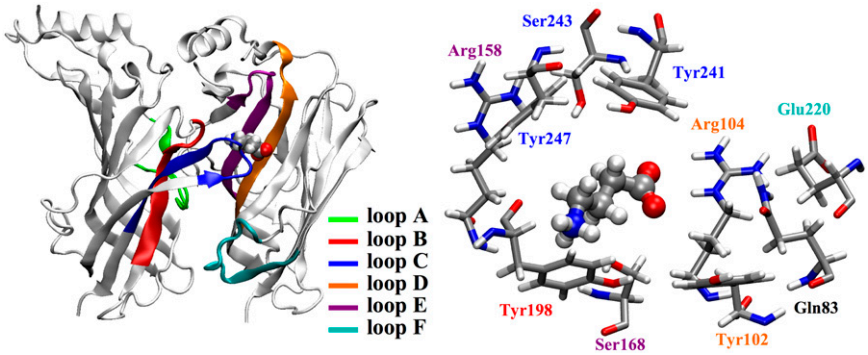

FIGURE 1 Two adjacent $GABA_C$ receptor subunits showing the orientation of GABA in the binding site after the initial minimization of the docked structure in the homology model. The ligand binding site consists of residues from loops *A–C* of one subunit and loops *D–F* of the adjacent subunit (*left*). A closeup of the binding pocket showing the residues referred to in this study (*right*); the residue labels are colored as the loops they belong to.

a cation-π interaction with an A-loop (rather than a B-loop) residue (11). In the $GABA_C$ receptor, both Arg^{104} and Arg^{158} have been shown, experimentally, to be important for binding and/or function, while in the $GABA_A$, receptor αArg^{66}, the residue equivalent to Arg^{104}, has been shown to be important for receptor function (12,13) and is proposed to form a part of a crown of arginines that stabilize the carboxylate group (14).

To explore the interactions of GABA in the binding site, we performed molecular dynamic (MD) simulations of a homology model of the $GABA_C$ receptor ECD in water to validate the homology model and assess the interactions of GABA inside the alleged binding site. We then focused on the role of Arg^{104} by mimicking previous mutagenesis experiments that evaluated how substitution with Ala, Glu, and Lys affected receptor function (6).

METHODS

For the classical molecular dynamics simulations we used the AMBER2003 force field (15) and the AMBER simulation package (16). The initial structure was the homology model for the $GABA_C$ receptor ECD with the neurotransmitter GABA docked in.

Briefly, using FUGUE (17), the sequence of the ρ_1 subunit of the human $GABA_C$ receptor was aligned to the AChBP sequence, based on the 2.7 Å resolution structure from *Lymnaea stagnalis* (18), as shown in Fig. 2. This is considered to be a ligand-bound structure and therefore is an appropriate template for ligand binding studies.

The three-dimensional models of the extracellular domain of the $GABA_C$ receptor were then built using MODELLER (19) by threading the aligned sequence over the crystal structure of AChBP. The most energetically favorable models were selected from the MODELLER output file using the ModelList program (http://www-cryst.bioc.cam.ac.uk/) and violations of the Ramachandran plot were checked using RAMPAGE (21). The homology model is similar to those previously reported for $GABA_C$ receptors (5–8), and also similar to $GABA_A$ receptor models (11,12).

Docking was performed using FLExX (BioSolveIT, Sankt Augustin, Germany). In particular, the docking model chosen is consistent with ''orientation 3'' in Harrison and Lummis (5), where GABA has its amine close to Tyr^{198}, its carboxylate close to Arg^{104}, and is within 5 Å from Arg^{158}; this was subtly different to the orientation of GABA obtained using a different docking program, where the carboxylate group was within 3 Å of Arg^{158} (6). Docking models are frequently inaccurate due to many simplifications used in their implementation, whereas MD simulations can provide considerably more accurate data as to the location of a ligand in a binding pocket by refining initial docking structures (22,23).

The use of classical molecular dynamics allowed us to simulate the whole extracellular domain; mutations with natural amino acids are also adequately described by the use of available classical force fields, while mutations with unnatural amino acids or unusual residues may require a treatment with ab initio techniques (24).

We used the program H++ (25) to evaluate the protonation state of the protein ionizable groups by calculating their pK_a shift with respect to the standard pK_a at neutral pH. After the protonation procedure, the total number of atoms was 16,915 and the total charge of the system was neutral. The GABA atomic partial charges were the ESP partial charges (26) calculated at a density functional theory level with the CPMD code (27), using the PBE gradient corrected functional for the exchange and correlation potential (28) and norm conserving Martins-Troulliers pseudopotentials (29), with a kinetic energy cutoff for the wavefunction expansion in plane waves of 70 Ry. The $GABA_C$ receptor ECD was surrounded by 18,314 TIP3P water molecules in a periodically repeated truncated octahedral box. To reproduce physiological conditions, 0.15 M dissociated KCl was added (equivalent to 49 K^+ ions and 49 Cl^- ions in our system). The electrostatic contributions were evaluated with the particle mesh Ewald method (30) using a cutoff for the direct space sum of 10 Å. We used an integration time step of 2 fs and constrained the bonds' length involving hydrogens with the SHAKE algorithm (31).

After a preliminary minimization, we equilibrated the system at constant temperature and pressure. First, we thermalized the solution at 310 K for 60 ps with a Langevin thermostat (32) with a collision frequency $\gamma = 1\ ps^{-1}$. Then we performed a 5 ns molecular dynamics simulation with the system coupled to a Berendsen thermostat at 310 K and a Berendsen barostat at 1 atm with coupling constants $\tau_T = 2$ ps and $\tau_P = 2$ ps, respectively (33). During the first nanosecond, we restrained the 20 (out of 209) amino acids closest to the transmembrane domain of each subunit to mimic the presence of the transmembrane domain. We then decreased the number of restrained residues from 20 to 10 for each subunit, to avoid restraints close to the GABA binding site, and equilibrated the system for further 4 ns. Finally we started a production run, which ran for 3.75 ns.

We analyzed the trajectory by evaluating the occurrence of the hydrogen bonds and cation-π interactions involving GABA. To identify the hydrogen bonds, we used as a criterion the distance between donor and acceptor ($<$3.5 Å) and the donor-hydrogen-acceptor angle ($>$120°). To identify the cation-π interactions, we used as a criterion the distance between the GABA amine nitrogen and the center of mass of the phenyl ring ($<$5 Å) and the angle between the normal to the phenyl ring and the vector pointing from the ring center of mass to the GABA amine nitrogen ($<$45°).

RESULTS AND DISCUSSION

Stability of the homology model and binding of GABA to the $GABA_C$ receptor

The root-mean-square displacement (RMSD) of the protein backbone (calculated with respect to the initial minimized

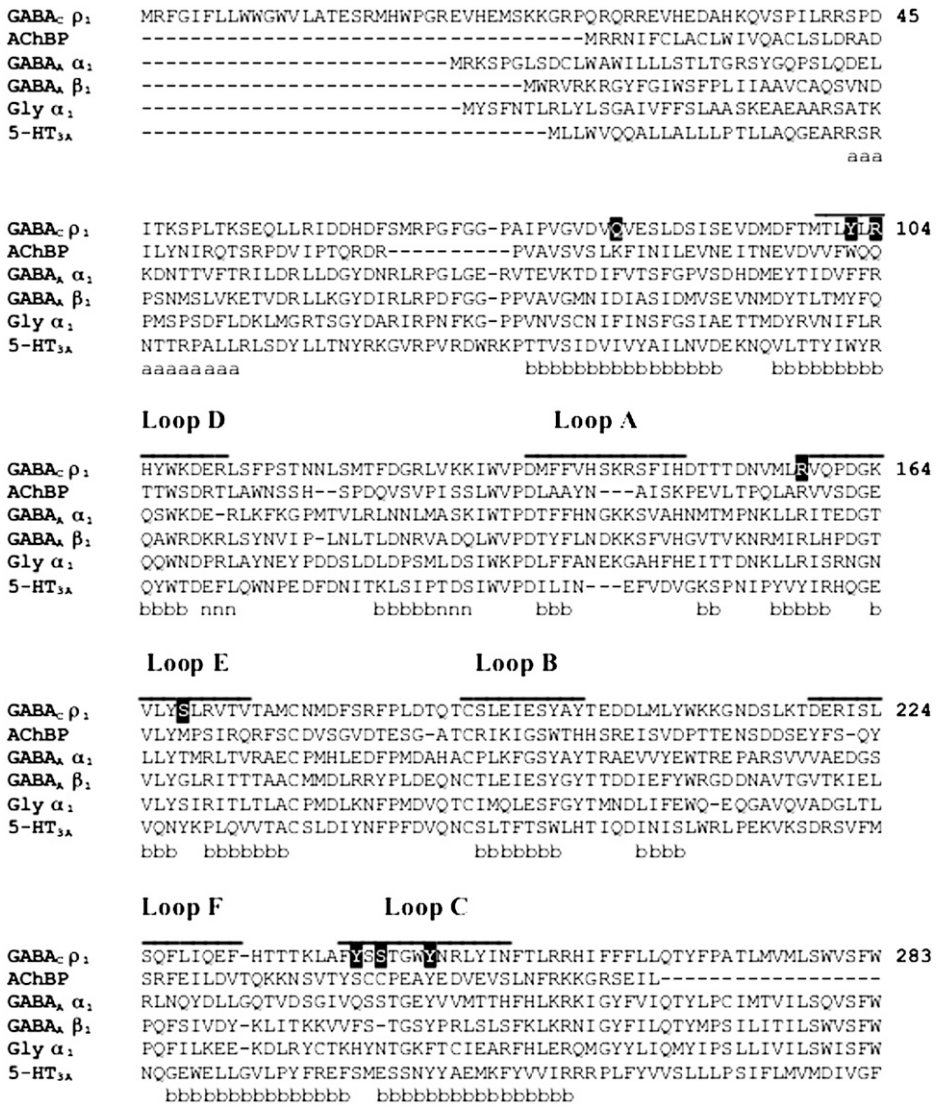

FIGURE 2 Multiple sequence alignment of representative $GABA_C$, AChBP, $GABA_A$, glycine, and 5-HT_{3A} receptor subunits ($GABA_C$ ρ_1 receptor subunit numbering). The binding loops *A–F* are indicated by lines above the alignment. The residues in the binding pocket shown in Fig. 2 are in solid boxes. Based on the secondary structure of AChBP, residues belonging to α-helices, β-sheets, and 3_{10}-helices are labeled with *a*, *b*, and *n*, respectively.

structure) is shown in Fig. 3 (*top*) together with the RMSD of the backbone of the residues in the binding pocket (*bottom*). These were defined as the residues within 10 Å from GABA in the minimized structure. The RMSD value stabilized at ~3 Å for both the protein and the binding site with only 10 out of 209 residues per subunits restrained. The homology model is therefore stable. Similar RMSDs were also calculated for the mutated receptors (34).

GABA remained bound to the $GABA_C$ receptor for the whole MD simulation. Its carboxylate group was always hydrogen-bonded to Arg^{104}, but the amine group was more mobile. During the first 2 ns of the production run, the amine group formed a cation-π interaction with Tyr^{102}, then GABA rapidly rotated ~100° to form a cation-π interaction with Tyr^{198}, as in the initial configuration. Two MD snapshots representative of the two orientations are shown in Fig. 4. Translations and rotations of GABA are shown in Fig. 5, where we monitored the distance between the position of the GABA center of mass at the beginning and at a generic time of the production run and the modulus of the angle between the lines passing through the center of mass and the amine nitrogen at the beginning and at a generic time of the production run. Very similar trends were found for the angle involving the carboxylate carbon rather than the amine nitrogen (34). Besides interacting with GABA, Arg^{104} formed on average 1.53 hydrogen bonds with Asp^{81} (equivalent to the sum of the time occurrence percentages of the hydrogen bonds between Arg^{104} and Asp^{81} divided by 100), of which 0.74 were as acceptor and 0.79 as donor.

Further binding partners of GABA were also identified in the two stable orientations. These were: Ser^{168}, which formed hydrogen bonds with the carboxylate group; Gln^{83} and Glu^{220}, which formed hydrogen bonds with the amine group, when GABA performed the cation-π interaction with Tyr^{102}; Ser^{243}, which formed hydrogen bonds with the carboxylate group; and Tyr^{198}, which formed hydrogen bonds with the amine group, when GABA performed the cation-π interaction with Tyr^{198}. Further details of the time occurrences of

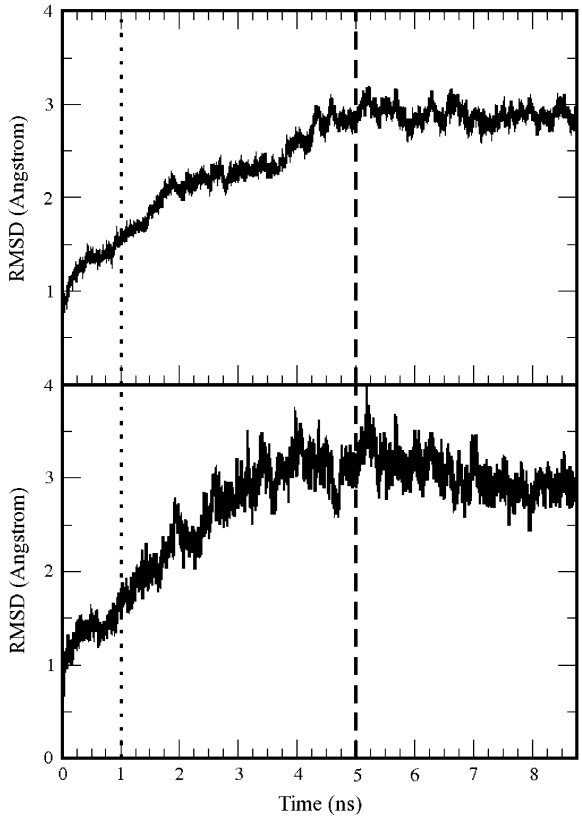

FIGURE 3 Root mean-square displacement of the protein backbone atoms (*top*) and of the backbone of the residues of the binding pocket (*bottom*) during the molecular dynamics. The residues of the binding pocket were defined as those with a distance of 10 Å from the initial position of GABA. The dotted line at 1 ns indicates when the restrained residues were reduced from 20 to 10 per subunit; the dashed line at 5 ns indicates the start of the production run.

these interactions are shown in Fig. 6. On average, the carboxylate group formed 1.67 hydrogen bonds with Arg^{104}, 0.53 with Ser^{243}, and 0.50 with Ser^{168}, while for the amine group the data show 0.34 with Gln^{83}, 0.33 with Tyr^{198}, 0.29 with Glu^{220}, 0.20 with Ser^{242}, and 0.14 with Tyr^{241} giving a total of 3.82 hydrogen bonds. GABA formed on average 0.31 cation-π interactions with Tyr^{102} and 0.41 with Tyr^{198}, giving a total of 0.72 cation-π interactions. These results suggest a possible conflict with the experimental data, which indicate a cation-π interaction only with Tyr^{198}. Tyr^{102} is clearly important, but has been proposed to be involved predominantly in gating but not binding (7). However, it may be that the interaction with Tyr^{102} is nonproductive, i.e., cannot result in gating, but is perhaps important for allowing GABA to interact with other residues, e.g., Ser^{168}, which has been shown to be important for binding (6,10).

We did not observe any bond of GABA with the other critical binding pocket arginine, Arg^{158}, during the whole simulation. In our initial configuration from the docking, both Arg^{104} and Arg^{158} were initially within 5 Å from GABA (considering any atom of the residues), which remained in the binding pocket for all the simulations, although the carboxylate group was closer to Arg^{104} and remained too far from the side groups of Arg^{158} to form hydrogen-bond interactions. While we cannot completely exclude some influence of the initial conditions, GABA was free to reorient itself and the system was equilibrated for a sufficiently long time to show whether Arg^{158} was a better binding partner than Arg^{104} for GABA. Thus we can infer that Arg^{104} has a more important role in binding GABA than Arg^{158}, although the latter does have a number of interactions as discussed below.

During the production run, Arg^{158} formed hydrogen bonds with other residues: on average 0.96 with Gln^{160}, 0.92 with Leu^{166}, and 0.18 with Ala^{199}. To test the effects of Arg^{158} mutations, we performed molecular dynamics simulations of the Arg^{158}Ala, Arg^{158}Glu, and Arg^{158}Lys mutant receptors, with the same simulation protocol used for the wild-type receptor. The hydrogen bond between the NH group of Leu^{166} and the oxygen of the carboxylic group of the residue at position 158 was maintained in all cases, with fairly high occurrences (92% for Arg^{158}, 96% for Ala^{158}, 80% for Glu^{158}, and 99% for Lys^{158}, which also acted as a donor through its NH group for another hydrogen bond with Leu^{166} with 61% occurrence). The side chain of the positively charged Arg^{158} and Lys^{158} formed a rather infrequent (18% in both cases) hydrogen bond with Ala^{199}, but only Arg^{158} interacted with Glu^{160}, with the three nitrogens of its side group acting, in turn, as donors for an average of 0.96 hydrogen bonds. The two oxygens of the negatively charged carboxylate group of Glu^{158} formed hydrogen bonds with Ser^{243} with an occurrence of 62% each, while the neutral side chain of Ala^{158} did not interact with any residue. The muta-

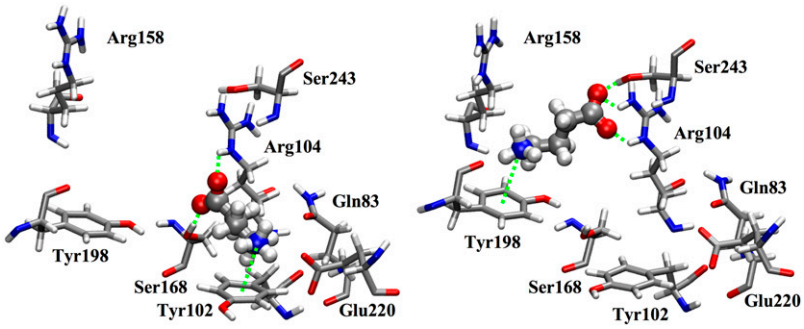

FIGURE 4 Two representative MD snapshots showing the two orientations of GABA during the simulation: on the left GABA forms hydrogen bonds with Arg^{104} and Ser^{168} and cation-π interactions with Tyr^{102}, while on the right it forms hydrogen bonds with Arg^{104} and Ser^{243} and cation-π interactions with Tyr^{198}.

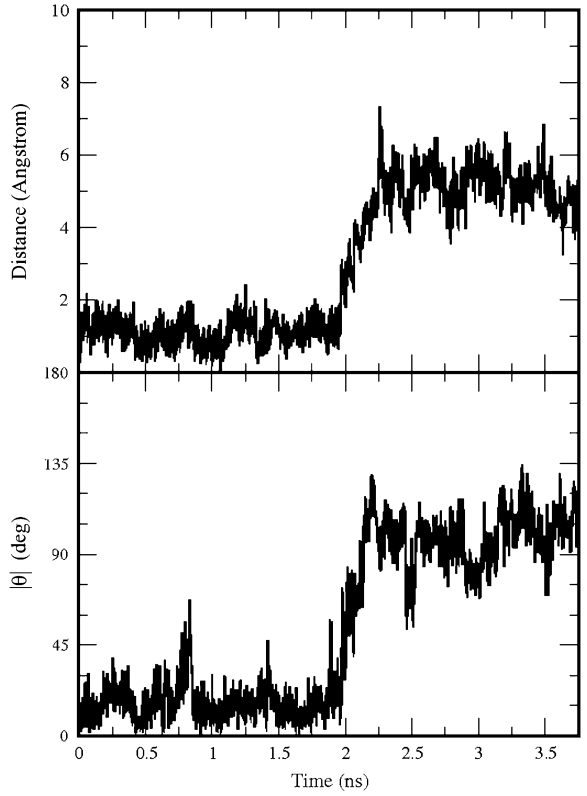

FIGURE 5 The distance of the GABA center of mass from its position at the beginning of the production run (*top*) in the $GABA_C$ receptor; the modulus of the angle θ between the lines passing through the GABA amine nitrogen and the GABA center of mass at the beginning and at a generic time of the production run (*bottom*).

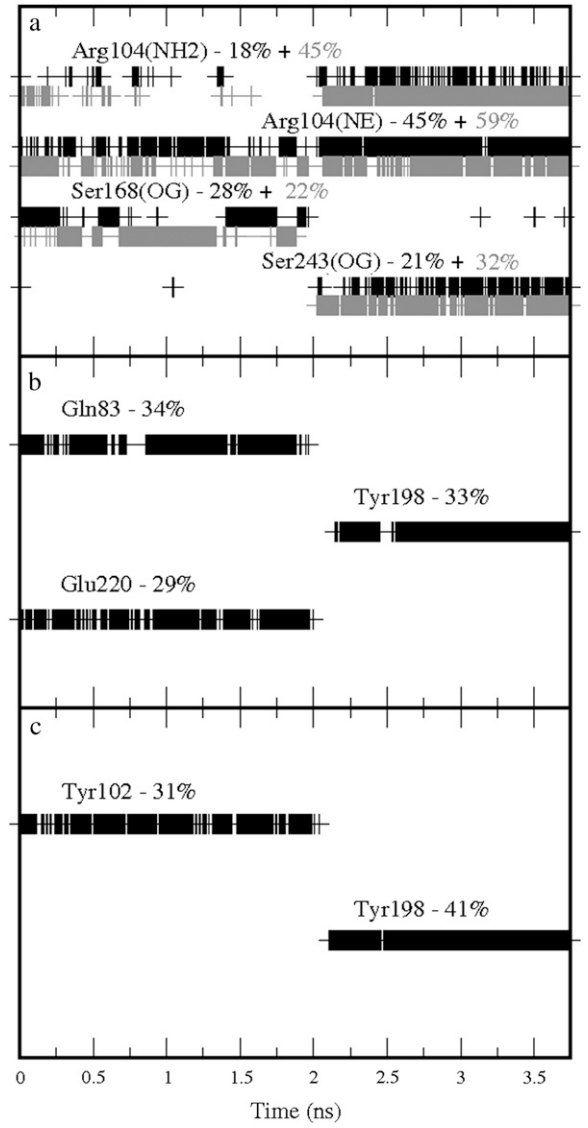

FIGURE 6 Time occurrences with the corresponding percentages over the production run of the bonds formed by GABA in the $GABA_C$ receptor: (*a*) Hydrogen bonds involving the GABA carboxylate group; the solid and shaded colors indicate the two oxygen atoms in the carboxylate group. (*b*) Hydrogen bonds involving the GABA amine group. (*c*) Cation-π interactions involving the GABA amine group. The labels used to indicate the atoms involved in the hydrogen bonds correspond to the atom types used in the AMBER package.

tions also indirectly affected the binding of GABA, in different ways for the different mutations. Specifically in the $Arg^{158}Lys$ receptor, the GABA carboxylate group did not bind to Arg^{104}. It formed, on average, 0.21 hydrogen bonds with Lys^{158}, 0.34 with Ser^{242}, 0.15 with Ser^{243}, and 0.09 with Ser^{168}; the GABA amine group maintained on average 0.32 cation-π interactions with Tyr^{198} and 0.49 hydrogen bonds with Tyr^{198}, 0.26 with Met^{156}, and 0.48 with Ser^{168}. In the $Arg^{158}Glu$ receptor, the GABA carboxylate group did interact with Arg^{104} (with an average of 1.37 hydrogen bonds, plus 0.89 and 0.96 hydrogen bonds with Ser^{168} and Ser^{242}, respectively), but the amine group did not form any cation-π interaction with Tyr^{198} or any other residues. It did, however, form hydrogen bonds with Glu^{158} (with an occurrence of 52%) and very infrequently with Ser^{243} (6%) and Glu^{168} (6%). In the $Arg^{158}Ala$ receptor, the GABA carboxylate group interacted with two of the nitrogen groups of the side chain of Arg^{104} (forming on average 2.50 hydrogen bonds), and with the two serines Ser^{168} and Ser^{243}, forming on average 0.97 and 0.14 hydrogen bonds, respectively; the GABA amine group also maintained a cation-π interaction with Tyr^{198} for 60% of the production run, and was also involved in, on average, 0.42 and 0.91 hydrogen bonds with Tyr^{247} and Leu^{166}, respectively. Thus our data suggest that the lack of function in the Arg^{158} mutant receptors is due to changes in the hydrogen-bond network, which could affect the binding of GABA and/or the links between the binding site and channel opening.

There has been a previous MD investigation of the extracellular domain of the $GABA_C$ receptor (8), based on a homology model built on a different structure of AChBP (from *Aplysia californica* at 2.02 Å resolution (35)). In this study, the chosen orientation of GABA from a docking procedure has similarities with ours: the GABA carboxylate group

forms a salt-bridge with Arg^{104} and the amine group interacts with Tyr^{198} and Tyr^{241}. A molecular dynamics study was performed for 7 ns on this structure, with partial solvation limited to sphere of 20 Å radius around the neurotransmitter, with the AMBER simulation package; it was found that GABA was very unstable in the binding site and interactions with important amino acids disappeared. In an additional simulation, where the docking procedure was performed on a structure obtained by a molecular dynamics equilibration, GABA was more stable with recorded interactions between the carboxylate group and Arg^{104}, although no quantitative information is available for comparison with our data.

Mutations of Arg^{104} with Ala, Glu, and Lys

To further test the role of Arg^{104} and to mimic previous experimental studies, we substituted Arg^{104} in each subunit in turn with Ala, Glu, and Lys in the homology model, and performed a new set of classical molecular dynamics simulations of the whole $GABA_C$ receptor extracellular domain in aqueous solution. The computational details, including the minimization and equilibration procedures and initial position of the ligand, were the same as for the wild-type receptor.

The substitution of the positively charged Arg with the neutral Ala produced a receptor with a total charge of $-5e$; hence, we added five positively charged (Na^+) counterions to neutralize the system. However, GABA was not stable in the binding pocket, and indeed, it completely exited the protein 4.6 ns into the equilibration. During the first ~3 ns of the equilibration, the GABA carboxylate group bound to Arg^{158}, confirming that this group preferred to bind to a positively charged residue. However, these hydrogen bonds were not as stable or as frequent as those previously formed by GABA and Arg^{104}, and indicate that Arg^{158} is a less favorable binding partner than Arg^{104}. The carboxylate group also formed infrequent bonds with Thr^{201} and Ser^{242}. The GABA amine group formed a cation-π interaction with Tyr^{198} and also a hydrogen bond with the carboxylic oxygen of Tyr^{198}. There were also infrequent hydrogen bonds with Met^{156}, Tyr^{200}, and Ser^{197}. After 3 ns of equilibration GABA oscillated inside the binding site for ~1 ns with very infrequent interactions and then left the binding site and the whole ECD. In the 4.6-ns equilibration MD simulation before GABA exited, the GABA carboxylate group formed, on average, 0.61 hydrogen bonds with Arg^{158}, 0.12 with Thr^{201}, and 0.06 with Ser^{242}; the GABA amine formed 0.33 hydrogen bonds with Tyr^{198}, 0.09 with Met^{156}, 0.12 with Tyr^{200}, and 0.11 with Ser^{197}. Ala^{104} formed, on average, 1.36 hydrogen bonds with Asp^{81}, of which 0.37 were as acceptor and 0.99 as donor.

The experimental data revealed a very large increase (~10,000-fold) in EC_{50} when Arg^{104} was substituted with Ala (6). These data are consistent with our simulation, which indicates that the stability of GABA inside the ECD dramatically decreased when Arg^{104} is replaced with Ala; indeed the decrease was so dramatic that GABA rapidly exited the binding site.

We then substituted the five subunits of the homology model with Glu at position 104. Glu has a negative charge of $-e$, hence the total charge of the system was $-10e$, and we added 10 counterions (Na^+) to neutralize the total charge. During the production run, GABA underwent large displacements and rotations, as seen in Fig. 7, which shows the distance between the positions of the GABA center of mass at the beginning and at a generic time of the production run (*top*), and the modulus of the angle between the lines passing through the center of mass and the amine nitrogen at the beginning and at a generic time of the production run (*bottom*).

In this simulation, the GABA carboxylate group found a new binding partner: Arg^{249}. Hydrogen bonds between the GABA carboxylate group and Arg^{249} (0.91 in the production run) were present intermittently for much of the simulation; however, these bonds were considerably less frequent than those with Arg^{104} in the wild-type receptor. The carboxylate group also formed, on average, 0.31 hydrogen bonds with Tyr^{241}, and the amine group formed infrequent hydrogen bonds with Tyr^{102} (0.15 on average) and Asp^{219} (0.16). In

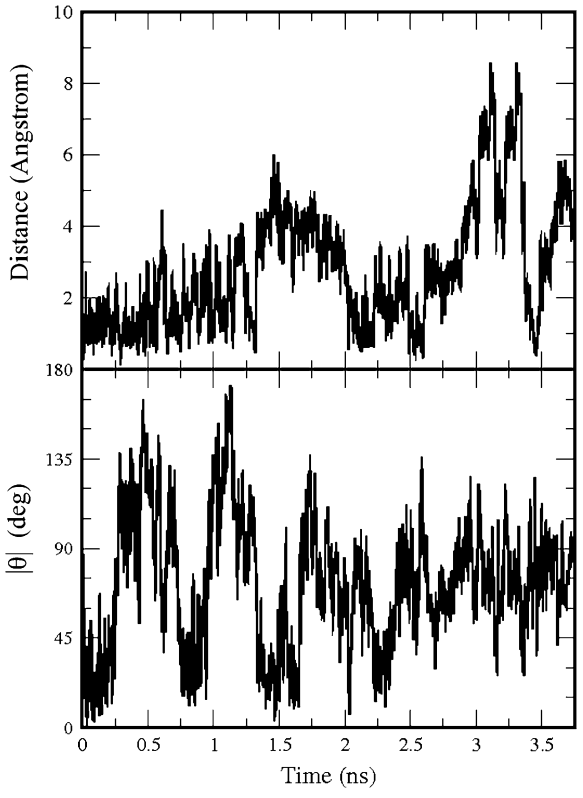

FIGURE 7 The distance of the GABA center of mass in the $Arg^{104}Glu$ $GABA_C$ receptor from its position at the beginning of the production run (*top*); the modulus of the angle θ between the lines passing through the GABA amine nitrogen and the GABA center of mass at the beginning and at a generic time of the production run (*bottom*).

summary, an average of 1.47 hydrogen bonds were formed. There were no cation-π interactions. Details of the time occurrences of these bonds can be seen in Fig. 8. Glu^{104} also formed, on average, 3.17 hydrogen bonds with Asp^{81} (0.96 as acceptor and 1.00 as donor), with Lys^{211} (1.13 as acceptor) and with Ser^{168} (0.08 as acceptor).

The experimental data revealed another large increase (~40,000-fold) in EC_{50} when Arg^{104} was substituted with Glu (6). Again the simulation indicates that the stability of GABA inside the ECD dramatically decreased when Arg^{104} was replaced with Glu; GABA formed, on average, significantly fewer bonds with the surrounding residues (1.47 hydrogen bonds and no cation-π interactions) than in the wild-type receptor. Interestingly, as in the previous simulation, GABA appeared to prefer to interact with another Arg, but in this case it was Arg^{249}, perhaps because this was more distant from the unfavorable negatively charged Glu.

Finally, we substituted Arg^{104} with Lys, which has the same positive charge; hence the total charge of the protein was neutral and we did not add any counterions. The distance between the position of the GABA center of mass at the beginning and at a generic time of the production run, and the modulus of the angle between the lines passing through the center of mass and the amine nitrogen at the beginning and at a generic time of the production run are shown in Fig. 9. GABA underwent relatively small rotations and overall remained reasonably close to its initial position. Unexpectedly, it only formed very infrequent (0.07) hydrogen bonds with Lys^{104}. It also formed 1.17 hydrogen bonds with Ser^{243}, 0.52 with Ser^{168}, 0.07 with Thr^{244}, and 0.07 with Ser^{242}. The amine group formed, on average, 0.30 and 0.22 hydrogen bonds with Tyr^{198} and Thr^{244}, and 0.32, 0.52, and 0.20 cation-π interactions with Tyr^{198}, Tyr^{241}, and Tyr^{247}, respectively. Details of the time occurrences of these bonds can be seen in Fig. 10. The average number of hydrogen bonds (2.42) is significantly smaller than for the wild-type receptor, while the number of cation-π interactions (1.14) is larger. Lys^{104} formed, on average, 2.13 hydrogen bonds with other residues of the $GABA_C$ receptor, of which 1.34 are with Asp^{81} (0.94 as acceptor and 0.40 as donor) and 0.79 are with Gln^{83} (as donor).

The experimental data showed that the receptor was insensitive to GABA up to a concentration of 30,000 μM when Arg^{104} was substituted with Lys. Our simulations suggest that the decrease in the number of hydrogen bonds and/or the

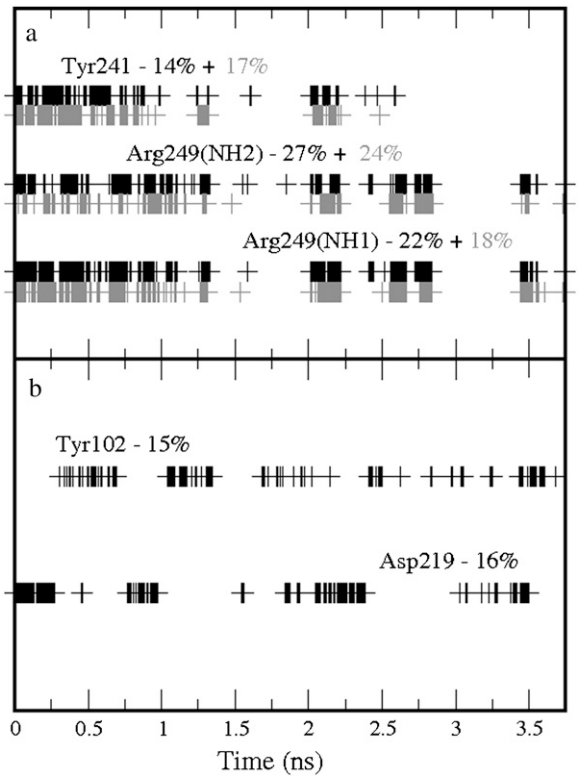

FIGURE 8 Time occurrences with the corresponding percentages over the production run of the bonds formed by GABA in the Arg^{104}Glu $GABA_C$ receptor: (*a*) Hydrogen bonds involving the GABA carboxylate group; the solid and shaded colors indicate the two oxygen atoms in the carboxylate group. (*b*) Hydrogen bonds involving the GABA amine group. No cation-π interactions were formed. The labels used to indicate the atoms involved in the hydrogen bonds correspond to the atom types used in the AMBER package.

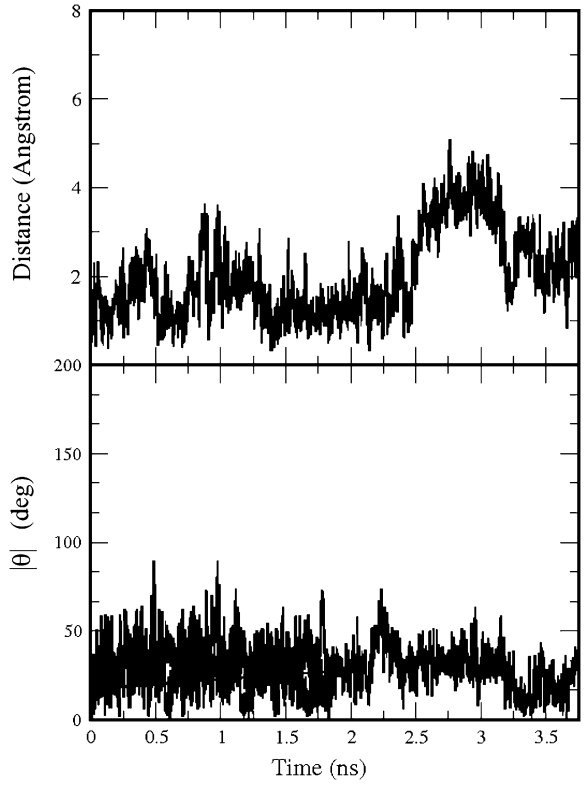

FIGURE 9 The distance of the GABA center of mass in the Arg^{104}Lys $GABA_C$ receptor from its position at the beginning of the production run (*top*); the modulus of the angle θ between the lines passing through the GABA amine nitrogen and the GABA center of mass at the beginning and at a generic time of the production run (*bottom*).

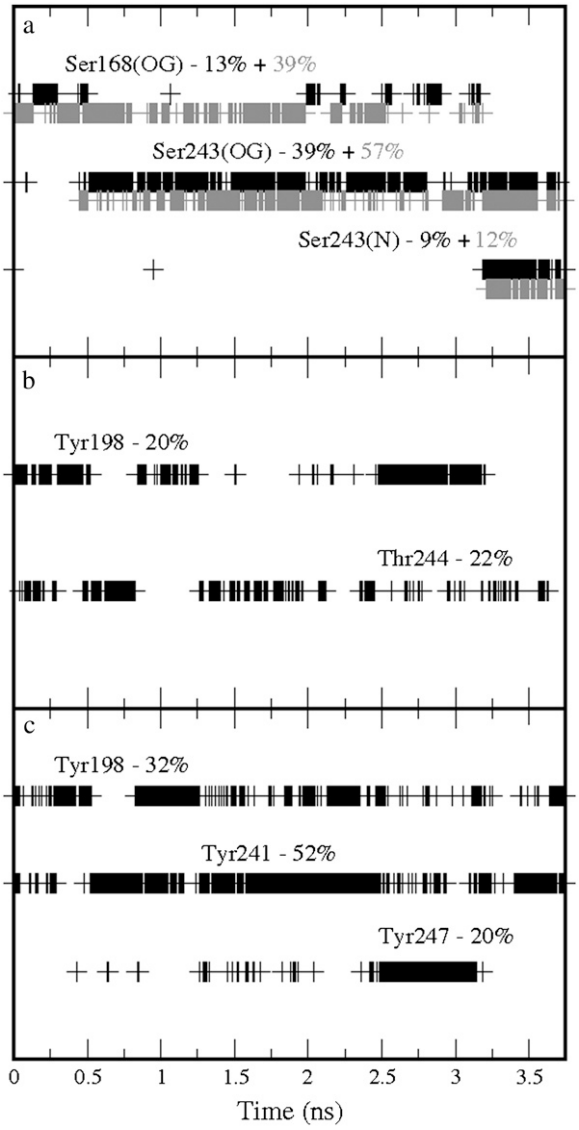

FIGURE 10 Time occurrences with the corresponding percentages over the production run of the bonds formed by GABA in the $Arg^{104}Lys$ $GABA_C$ receptor: (*a*) Hydrogen bonds involving the GABA carboxylate group; the solid and shaded colors indicate the two oxygen atoms in the carboxylate group. (*b*) Hydrogen bonds involving the GABA amine group. (*c*) Cation-π interactions involving the GABA amine group. The labels used to indicate the atoms involved in the hydrogen bonds correspond to the atom types used in the AMBER package.

lack of interaction with Lys^{104} renders GABA incapable of interacting sufficiently in the binding pocket to open the channel.

In conclusion, the data from the simulations strongly support the experimental data in suggesting a critical role for Arg^{104}. The simulation with the wild-type receptor revealed hydrogen bonds between this residue and GABA for much of the simulation, but GABA formed extremely infrequent ($<1\%$) bonds when this residue was mutated to Lys and no bonds at all when it was mutated to Ala or Glu.

C. Melis and C. Molteni thank the Engineering and Physical Sciences Research Council Life Science Interface Program for financial support (grant No. EP/E014505/1). S. C. R. Lummis is a Wellcome Trust Senior Research Fellow in Basic Biomedical Science.

REFERENCES

1. Bormann, J. 2000. The ''ABC'' of GABA receptors. *Trends Pharmacol. Sci.* 21:16–19.
2. Barnard, E. A., P. Skolnick, R. W. Olsen, H. Moher, W. Sieghart, G. Biggio, C. Braestrup, A. Bateson, and S. Z. Langer. 1998. International union of pharmacology. XV. Subtypes of γ-Aminobutyric $Acid_A$ receptors: classification on the basis of subunit structure and receptor function. *Pharmacol. Rev.* 50:291–314.
3. Chebib, M., and G. A. R. Johnston. 2000. GABA-activated ligand gated ion channels: medicinal chemistry and molecular biology. *J. Med. Chem.* 43:1427–1447.
4. Enz, R. 2001. $GABA_C$ receptors: a molecular view. *Biol. Chem.* 382:1111–1122.
5. Harrison, N. J., and S. C. R. Lummis. 2006. Molecular modeling of the $GABA_C$ receptor ligand-binding domain. *J. Mol. Model.* 12:317–324.
6. Harrison, N. J., and S. C. R. Lummis. 2006. Locating the carboxylate group of GABA in the homomeric $\rho GABA_A$ receptor ligand-binding pocket. *J. Biol. Chem.* 281:24455–24461.
7. Sedelnikova, A., C. D. Smith, S. O. Zakharkin, D. Davis, D. S. Weiss, and Y. Chang. 2005. Mapping the $\rho 1$ $GABA_C$ receptor binding pocket. *J. Biol. Chem.* 280:1535–1542.
8. Osolodkin, D. I., V. I. Chupakhin, V. A. Palayulin, and N. Z. Zefirov. 2007. Modeling and analysis of ligand-receptor interactions in the $GABA_C$ receptor Dokl. *Biochem. Biophys.* 412:25–28.
9. Krishek, B. J., A. Amato, C. N. Connolly, S. J. Moss, and T. G. Smart. 1996. Proton sensitivity of the $GABA_A$ receptor is associated with the receptor subunit composition. *J. Physiol.* 492:431–443.
10. Lummis, S. C. R., D. L. Beene, N. J. Harrison, H. A. Lester, and D. A. Dougherty. 2005. A cation-π interaction with a tyrosine in the binding site of the $GABA_C$ receptor. *Chem. Biol.* 12:993–997.
11. Padgett, C. L., A. P. Hanek, H. A. Lester, D. A. Dougherty, and S. C. R. Lummis. 2007. Unnatural amino acid mutagenesis of the $GABA_A$ receptor binding site residues reveals a novel cation-π interaction between GABA and $\beta_2 Tyr^{97}$. *J. Neurosci.* 27:886–892.
12. Holden, J. H., and C. Czajkowski. 2002. Different residues in the $GABA_A$ receptor α_1T60-α_1 K70 region mediate GABA and SR-95531 actions. *J. Biol. Chem.* 277:18785–18792.
13. Hartvig, L., B. Lukensmejer, T. Liljefors, and K. Dekermendjian. 2000. Two conserved arginines in the extracellular N-terminal domain of the $GABA_A$ receptor $\alpha 5$ subunit are crucial for receptor function. *J. Neurochem.* 75:1746–1753.
14. Wagner, D. A., C. Czajkowski, and M. V. Jones. 2004. An arginine involved in GABA binding and unbinding but not gating of the $GABA_A$ receptor. *J. Neurosci.* 24:2733–2741.
15. Ponder, J. W., and D. A. Case. 2003. Force fields for protein simulations. *Adv. Protein Chem.* 66:27–85.
16. Case, D. A., T. E. Cheatham III, T. Darden, H. Gohlke, R. Luo, K. M. Merz, Jr., A. Onufriev, C. Simmerling, B. Wang, and R. J. Woods. 2005. The AMBER biomolecular simulation programs. *J. Comput. Chem.* 26:1668–1688.
17. Shi, J., T. L. Blundell, and K. Mizuguchi. 2001. FUGUE: sequence-structure homology recognition using environment-specific substitution tables and structure-dependent gap penalties. *J. Mol. Biol.* 310:243–257.
18. Brejc, K., W. J. V. Dijk, R. V. Klassen, M. Schuurmans, J. van Der Oost, A. B. Smith, and T. K. Sixma. 2001. Crystal structure of an ACh-binding protein reveals the ligand-binding domain of nicotinic receptors. *Nature*. 411:269–276.
19. Sali, A., and T. L. Blundell. 1993. Comparative protein modeling by satisfaction of spatial restraints. *J. Mol. Biol.* 234:779–815.

20. Reference deleted in proof.

21. Lovell, S. C., I. W. Davis, W. B. Arendall III, P. I. W. de Bakker, J. M. Word, M. G. Prisant, J. S. Richardson, and D. C. Richardson. 2003. Structure validation by Cα geometry: ϕ, ψ and Cβ deviation. *Proteins Struct. Funct. Genet.* 50:437–450.

22. Leach, A. R., B. K. Shoichet, and C. Peishoff. 2006. Prediction of protein-ligand interactions. Docking and scoring: successes and gaps. *J. Med. Chem.* 49:5851–5855.

23. Warren, G. L., C. W. Andrews, A.-M. Capelli, B. Clarke, J. LaLonde, M. Lambert, M. Lindvall, N. Nevins, S. F. Semus, S. Senger, G. Tedesco, I. Wall, J. M. Woolven, C. E. Peishoff, and M. Head. 2006. A critical assessment of docking programs and scoring functions. *J. Med. Chem.* 49:5912–5931.

24. Melis, C., P.-L. Chau, K. L. Price, S. C. R. Lummis, and C. Molteni. 2006. Exploring the binding of serotonin to the 5–HT3 receptor by density functional theory. *J. Phys. Chem. B.* 110:26313–26319.

25. Gordon, J. C., J. B. Myers, T. Folta, V. Shoja, L. S. Heath, and A. Onufriev. 2005. H++: a server for estimating pK_as and adding missing hydrogens to macromolecules. *Nucleic Acids Res.* 33:368–371.

26. Singh, U. C., and P. A. Kollman. 1984. An approach to computing electrostatic charges for molecules. *J. Comput. Chem.* 5:129–145.

27. CPMD, Ver. 3.11. Copyright IBM Corp. 1990–2006. Copyright MPI für Festkörperforshung Stuttgart 1997–2001.

28. Perdew, J. P., K. Burke, and M. Ernzerhof. 1996. Generalized gradient approximation made simple. *Phys. Rev. Lett.* 77:3865–3868.

29. Troullier, N., and J. L. Martins. 1991. Efficient pseudopotentials for plane-wave calculations. *Phys. Rev. B.* 43:1993–2006.

30. Allen, M. P., and D. J. Tildesley. 1987. Computer Simulation of Liquids. Oxford University Press, Oxford, UK.

31. Ryckaert, J. P., G. Ciccotti, and H. J. C. Berendsen. 1977. Numerical integration of the Cartesian equations of motions of a system with constraints: molecular dynamics of *n*-alkanes. *J. Comput. Phys.* 23: 327–341.

32. Adelman, S. A., and J. D. Doll. 1976. Generalized Langevin equation approach for atom/solid-surface scattering: general formulation for classical scattering off harmonic solids. *J. Chem. Phys.* 64:2375–2388.

33. Berendsen, H. J. C., J. P. M. Postma, W. F. van Gusteren, A. D. Nola, and J. R. Haak. 1984. Molecular dynamics with coupling to an external bath. *J. Chem. Phys.* 81:3684–3690.

34. Melis, C. 2007. Mutagenesis computer experiments on ligand-gated ion channels. PhD thesis, King's College London, London, UK.

35. Hansen, S. B., G. Sulzenbacher, T. Huxford, P. Marchot, P. Taylor, and Y. Bourne. 2005. Structures of *Aplysia* AChBP complexes with nicotinic agonists and antagonists reveal distinctive binding interfaces and conformations. *EMBO J.* 24:3635–3646.